Original Research Article

GREENHOUSE GASES SCIENCE AND TECHNOLOGY

Energy and economic analysis feasibility of CO_2 capture on a natural gas internal combustion engine

Alexander García-Mariaca and Eva Llera-Sastresa, University of Zaragoza, Zaragoza, Spain

Abstract: CO_2 capture by amine scrubbing is a widely developed technology in its most advanced stage of evolution. However, it has never been used to capture CO_2 from mobile sources. The present study performs an energy and economic analysis of an amine scrubbing CO_2 capture storage (CCS) system, which takes for the amine regeneration process the waste heat from the exhaust gases of a turbocharged natural gas internal combustion engine (mobile source). The selected engine for the study is an M936G, widely used in freight and passenger transport. A primary and a tertiary amine were chosen for the simulations. In order to reduce volume and increase autonomy, captured CO_2 is stored as a liquid, therefore, a specific installation is planned. The system is hybridised with an organic rankine cycle (ORC) to reduce the energy penalty on the CCS system. Results show that a CCS system operating with Monoethanolamine (MEA) at 30 wt% achieved a maximum CO_2 capture rate of 66%, with a penalty over the power engine of only 10%. On the other hand, the economic analysis showed that the CCS system with MEA and without ORC is 31.8% cheaper than a hydrogen fuel cells bus and 26% cheaper than a battery-electric bus. © 2022 Society of Chemical Industry and John Wiley & Sons, Ltd.

Keywords: CO_2 capture; amine-scrubbing; internal combustion engines; organic Rankine cycle

Introduction

Currently, the transport sector contributes 25% of total CO_2 emissions and is gradually migrating towards electrification to reduce its CO_2 footprint.[1] However, in freight and passenger transport, battery electric vehicles (BEV) and fuel cell vehicles (FCV) can only be a supplement, but not an alternative, to classic combustion engines,[2] due to short autonomies. This sector is expected to continue operating with C-H chain fuels, and thus the challenge focuses on fuels such as natural gas or synthetic natural gas. If, as in this last case, CH_4 is elaborated with a CO_2 captured (in an onboard Internal combustion engine vehicle) as raw material and an energy surplus from renewable sources, it could close the gap and drive the transport sector towards zero CO_2 emissions.

CCS is a potential technology for sustainable energy production and reducing CO_2 emissions.[3,4] The CCS systems allow CO_2 to be separated from a gas stream before or after a combustion process.[5] These technologies have mainly been applied in the heat and power generation sector and industries, such as cement and steel production.[6] In particular, CO_2 capture technologies in post-combustion have had significant advances in recent years. Whereby the use of these

Correspondence to: Alexander García-Mariaca, Escuela de Ingeniería y Arquitectura, University of Zaragoza, María de Luna s/n, Zaragoza, 50018, Spain.
Email: alexander.garcia@unizar.es
Received May 30, 2022; revised July 28, 2022; accepted August 1, 2022
Published online at Wiley Online Library (wileyonlinelibrary.com). DOI: 10.1002/ghg.2176

technologies in the transport sector could be functional. Some authors suggest that amine scrubbing, adsorption and membranes could be adapted to operate on mobile sources.[7,8]

So far, the research about CCS systems in mobile sources has been focused on absorption and adsorption. Engine-driven ships offer the most favourable scenario for an absorption installation because the internal combustion engine (ICE) operates almost at the same load condition in a journey, which is quite like the operating conditions of a power plant. Ship-based carbon capture (SBCC) research works have focused on amine scrubbing facilities. They have made economic analyses and evaluated several amines in different proportions, CO_2 capture rates (CCR) and the use of waste energy recovery systems.

For instance, Awoyomi *et al.*[9] studied the effect of exhaust gas recirculation (EGR) on an liquefied natural gas (LNG)-fuelled ship. They obtained a CCR of 90% with a solvent of NH_3 in a concentration of 4 wt% and solvent flow close to 40 kg/s. Stec *et al.*[10] evaluated in a diesel-fuelled ship an amine-scrubbing facility under three atmospheric conditions (arctic, ISO and tropical) using a solvent with Monoethanolamine (MEA) at 30 wt%. The best results were found under tropical conditions with values of CCR of 91.4%, 2.249 MW of heat duty and a regeneration heat of 3.61 MJ/kgCO_2. Güler and Ergin,[11] in several LNG-fuelled ships, evaluated an amine-scrubbing facility with a solvent concentration of 35 wt% of MEA. The average result of CCR obtained in their study was 33%. Ros *et al.*[12] evaluated SBCC on 12 LNG-fuelled engines (8 MW each) with a solvent of 30 wt% of MEA. The main results were a maximum CCR of 81% with an average price of 125 €/CO_2ton (depending on the storage pressure of CO_2). Luo and Wang,[13] in a diesel-fuelled ship of 10.8 MW with a waste energy recovery system (WERS), made an economic analysis of an amine-scrubbing plant using MEA at 30 wt% as solvent. The results show a CCR of 73% and a CO_2 capture price of 77.5 €/CO_2ton without the WERS. With WERS, 90% of CCR is reached with a higher CO_2 capture price of 163 €/CO_2ton. Feenstra *et al.*[14] evaluated two solvents, MEA and piperazine (PZ), for the CO_2 capture process on a 3 MW LNG-fuelled ship. The main conclusion of their study is that the cost of CO_2 capture is 120 €/CO_2ton using MEA and 98 €/CO_2ton using PZ.

In contrast, in ICE vehicles (ICEv), their rapid accelerations and decelerations and changes in the speed and load in the engine are the bottlenecks that do not allow the implementation of CCS systems in this sector. The research works found in the literature have evaluated the energy requirements of the CCS system and the most suitable sorbent or solvent. Sharma and Maréchal[15] elaborated an energy analysis of a CCS system by temperature swing adsorption (TSA) on a diesel-fuelled engine of a truck. The main result obtained is that with a WERS taking the thermal energy exhaust gases in advantage and with PPN-6-CH2-TETA as sorbent, the CCS system does not have penalisation over the ICE with a CCR of 90%. García and Llera[5] presented an energy analysis of a CCS system with TSA operating with several sorbents. The CCS system is hybridised with an organic Rankine cycle (ORC) to supply the utilities of the CCS system. The main conclusion obtained is a 73% of CCR with MOF-74-Mg without penalisation over the engine.

Regarding absorption, Kumar *et al.*[16,17] evaluated MEA, methyl diethanolamine (MDEA) and blends with NH_3 on a diesel-fuelled engine. The main result of these investigations is that MEA has a CO_2 reduction overcome 90% in any engine load condition. However, these research works do not describe how the regeneration process of the solvent in the CO_2 capture unit would be.

As shown above, CO_2 capture by absorption in ICEv has a few scientific developments, and this study aims to broaden the knowledge of this field. This research paper presents the first thermo-economic study of a CCS system onboard a natural gas (NG)-fuelled vehicle operating in the entire rpm operating range and under four engine load conditions. The CCS system proposed is subject to a sensitivity analysis using a primary and tertiary amine with 30 wt% in the solvent. Evaluations are carried out also with the hybridisation of an ORC that takes the exhaust gases' thermal energy to supply the amine-scrubbing and CO_2 compression utilities. The simulation of the different processes was carried out in Aspen Plus. The feasibility analysis aims at answering the following questions: (i) Is the intended heat integration of the exhaust gases with the CCS systems and ORC thermally feasible? (ii) What is the maximum CCR with the primary and tertiary amines? (iii) How much is the purchase cost of a vehicle with a CCS system installed? (iv) What is the power penalisation of the CCS over the engine performance?

Table 1. Technical specifications of the M936G engine.[20]

Architecture	In-line 6-cylinder engine
Aspiration method	Turbocharged with Aftercooler
Injection	Multipoint
Valves per cylinder:	4
Bore [mm]	110
Stroke [mm]	135
Displacement volume [cm^3]	7700
Compression ratio	17
Brake Power [kW]	222 at 1950 rpm
Torque [Nm]	1200 at 1600 rpm

Methodology

The energy analysis of CO_2 capture on board an ICEv through amine scrubbing developed in this research involves integrating three systems: the ICE (CO_2 generator), the CCS system and the WERS. Ideally, the thermal energy required for CO_2 desorption should come from the exhaust gases of the vehicle's engine, and the electricity for the operation of the CCS system devices should come from the engine and from the WERS, which in the case of this study will be an ORC. After technical analysis, an economic analysis is performed. The evaluated total capital expenditure (CAPEX) will be used to establish whether the hybridisation of these three systems in an ICEv for CO_2 reduction is competitive with other CO_2 reduction technologies available in the market. Each component and procedure developed in the simulations are described below.

Engine selection and model

Engine selection

In the short and medium term, ICEvs will keep using carbon-based fuels while the transport sector migrates completely towards electrification. Gaseous fuels such as natural gas (mainly CH_4) will be one of the best choices because of the high lower heating value (LHV) and short carbon chain that produces less CO_2.[18,19] On this basis, a heavy-duty turbocharged natural gas (NG) spark ignition (SI) engine of reference M936G has been selected to run the simulations. This engine is widely used in trucks and buses. The technical specifications of the engine are summarised in Table 1.

Engine simulation

The selected SI-ICE is simulated over AVL BOOST software to determine the pressure, temperature and concentration of the engine exhaust gases at the catalytic converter outlet. The simulations were performed at four engine load conditions (25, 50, 75 and 100%) in the rotational speed range of 1000–1900 rpm. The models used in the simulations are the Heywood, Patton and Nitschke model for the friction, the Woschni heat transfer model for the heat transfer in the cylinders, and the re-analogy for the heat transfer in the engine ducts. Finally, the air inlet is at standard conditions. The main input parameters to run the simulations are listed in Table 2.

Engine model validation

The results of brake power (BP) and brake-specific fuel consumption (BSFC) obtained in the simulations are validated with the values given by the manufacturer for these variables.[20] As can be seen in Table 3, the maximum error between the simulation and the manufacturer values is 6.63%. Therefore, the results obtained in the engine simulation present an appropriate behaviour, considering that the pressure, temperature, concentration and exhaust gases mass flow are close to reality.

Model development of the amine-scrubbing and CO_2 compression facilities

Amine selection

Amines are organic compounds which have been used for CO_2 capture since the 1930s becoming a widely used effective method in the industry.[24] They are usually diluted in water in concentrations up to 30 wt%. Primary and secondary amines react with CO_2 to produce ammonium carbamates through the formation and deprotonation of zwitterion, as described in reactions 1 and 2.[25]

$$R_1R_2NH + CO_2 \rightarrow R_1R_2NH^+COO^- \quad \text{(R1)}$$

$$R_1R_2NH^+COO^- + R_1R_2NH \rightarrow R_1R_2NCOO^- + R_1R_2NH_2^+ \quad \text{(R2)}$$

Tertiary amine reaction does not form zwitterion. Tertiary amines produce an unstable carbamate, and an additional reaction leads to the generation of

Table 2. Input parameters in AVL BOOST for the engine simulations.

Variable	Unit	M936G
Firing Order	NA	1,5,3,6,2,4
Star of combustion	CAD	−18
Combustion duration	CAD	57
A/F ratio	—	Stoichiometric combustion [16.75]
Maximum boost pressure ratio	—	2
Connecting Rod Length	mm	250
Lower heating value NG[21–23]	MJ/kg	48351

Table 3. Comparison engine results between the simulation and manufacturer chart.

Engine load [%]	rpm	Real[20]		Simulation		Error	
		BP [kW]	BSFC [g/kWh]	BP [kW]	BSFC [g/kWh]	BP [%]	BSFC [%]
100%	1000	110.0	200.00	110.17	192.04	-0.2%	4.0%
	1400	181.0	186.00	174.98	187.81	3.3%	−1.0%
	1600	204.0	188.00	197.27	188.33	3.3%	−0.2%
	1900	220.0	193.00	227.45	189.60	−3.39%	1.76%
75%	1000	82.5	225.00	82.91	221.52	−0.50%	1.54%
	1400	135.75	209.25	136	209.19	−0.18%	0.03%
	1600	153	211.50	153.6	211.57	−0.39%	−0.03%
	1900	165	217.13	166.3	217.29	−0.79%	−0.08%
50%	1000	55	270.00	55.26	269.47	−0.47%	0.19%
	1400	90.5	251.10	96.5	246.57	−6.63%	1.80%
	1600	102	253.80	104.36	253.61	−2.31%	0.07%
	1900	110	260.55	112.45	260.77	−2.23%	−0.09%
25%	1000	27.5	416.00	27.42	421.00	0.29%	−1.20%
	1400	45.25	386.88	45.26	387.11	−0.02%	-0.06%
	1600	51	391.04	50.69	391.21	0.61%	−0.04%
	1900	55	401.44	54.01	401.36	1.80%	0.02%

bicarbonate ions (reaction 3). This reaction increases theoretical CO_2 loading compared to primary and secondary amines.[26]

$$R_1R_2R_3N + H_2O + CO_2 \rightarrow R_1R_2R_3NH^+HCO_3^- \quad (R3)$$

According to the literature, primary amines require more regeneration energy than tertiary amines.[27] The reported value for MEA is 5 MJ/kg_{CO2}, while MDEA presents values of 2.8 MJ/kg_{CO2} with stripper temperatures between 100 and 120°C.[28] A similar behaviour presents the CO_2 loading capacity with values close to 0.6 mol_{CO2}/mol_{amine} for amine primaries[29] and 0.7 mol_{CO2}/mol_{amine} for tertiary amines.[30] Despite this, primary and secondary amines are mainly used because carbamate formation exceeds those of bicarbonate. Several research works display that reaction constant can vary from 47740 m^3/s/kmol for DETA[31] to 8400 m^3/s/kmol for MEA[32] and 11.15 m^3/s/kmol for MDEA.[30] Table 4 shows the main physical–chemical properties of the amines at a concentration of 30 wt%.

In the present research, a primary amine (MEA) and a tertiary amine (MDEA) have been selected to compare the maximum CO_2 capture rate (CCR).

Table 4. Amine properties at 30wt% and 313 K.

Solvent	Rate constant reaction [m^3/kmol/s]	Absorption heat [kJ/$kmol_{CO2}$]	CO_2 loading [$molCO_2/mol_{amine}$]	Reference
Ethanolamine (MEA)	8400	85.13	0.59	29, 33
Diethanolamine (DEA)	1340	74.24	0.61	29, 33, 34
Triethylamine (TEA)	16.8	66.59	0.38	29, 33, 34
Piperazine (Pz)	53700	80.58	0.91	35, 36
Aminomethyl propanol (AMP)	21000	80.91	0.78	29, 33, 34
Methyl diethanolamine (MDEA)	11.5	52.51	0.74	30, 37
Diethylenetriamine (DETA)	47000	89.48	1.414	38, 39, 40

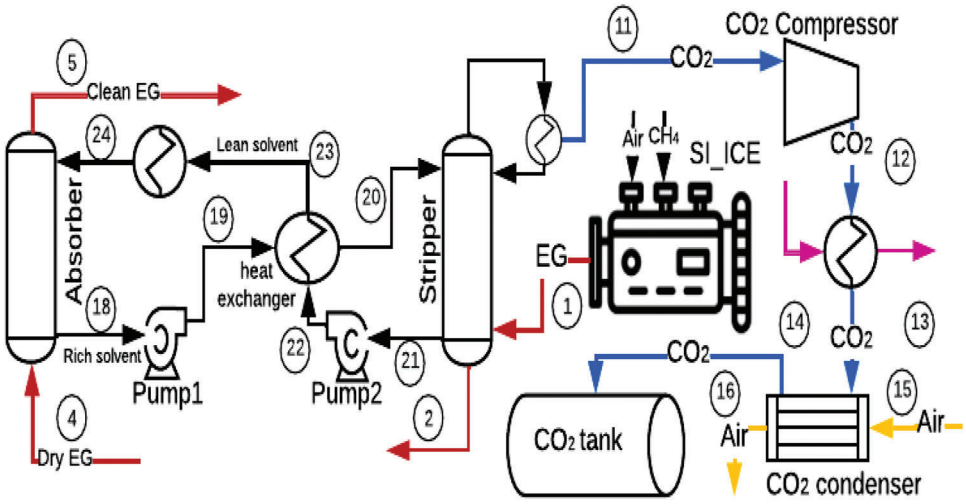

Figure 1. Amine-scrubbing and CO_2 compression facilities diagram.

Capture rates are expected to depend on the variation of engine rotational speed and engine load conditions. The regeneration heat is obtained employing Eqn 1, which relates to the heat given up by the exhaust gases in the stripper (see Fig. 1) and the CO_2 mass captured.

$$Q_{\text{regeneration}} = \frac{Q_{\text{exhaust gases}}}{m_{CO_2-\text{storage}}} \quad (1)$$

CCS configuration

According to the literature, amine scrubbing has a great potential to be used as a technique of CO_2 capture onboard ICEv:[7] Fig. 1 displays the amine scrubbing facility and the CO_2 compress process diagram. The exhaust gases from the ICE are used to heat the stripper and produce solvent regeneration (1, Fig. 1). The desorption temperature is set to 120°C to avoid corrosion problems and high solvent degradation. A pinch delta temperature of 10°C is assumed, whereby the exhaust gases at the stripper outlet are fixed to be 130°C (2, Fig. 1)(). After releasing heat in the ORC, the exhaust gases are cooled down and dried to 40°C before entering the bottom absorber (4, Fig. 1). The lean solvent enters at the top of the column (24, Fig. 1). The countercurrent flows of solvent and exhaust gases react in the absorber. The clean exhaust gas leaves the absorber at the top (5, Fig. 1). Rich solvent leaves the column at the bottom (18, Fig. 1), and it is pumped to the heat exchanger (19, Fig. 1), where the temperature is raised to 87°C before entering the top of the stripper (20, Fig. 1). Lean solvent abandons at 101°C and then goes to the heat exchanger and thus transfers thermal energy to the rich solvent (21-22, Fig. 1), reducing its temperature to 84°C. The lean solvent is cooled down until 40°C in a cooler before entering again in the absorber (23-24, Fig. 1). Finally, the water content in CO_2 flow is removed in the condenser, and high purity CO_2 gas flow goes to the compression stage (11, Fig. 1). Table 5 summarised the parameters assumed in the

Table 5. Parameters of the amine-scrubbing and CO_2 compression devices assumed in the simulations.

Device	Parameter	Value	Reference
Stripper	Operating temperature	120°C	41
Absorber	Operating temperature	40°C	42
Pumps 1 and 2	Isentropic efficiency	0.55	43
CO_2 Compressor	Isentropic efficiency	0.65	43

Table 6. Parameter values for the calculation of the inlet pressure to the expander.

Variable	Value	Unit
Compressibility factor (Z)	0.73	NA
R	0.1186	kJ/kg·K
T_{sat} at 25% of engine load (6.8 bar)	395.13	K
ΔT_{SH} at 25% engine load (6.8 bar)	0	K
ΔT_{SH} at 50% engine load (6.8 bar)	10	K
ΔT_{SH} at 75% engine load (6.8 bar)	23	K
ΔT_{SH} at 100% engine load (6.8 bar)	39	K
$\rho_{pump,in}$ at 1 bar (saturated liquid)	735.3	kg/m^3
$\eta_{vol,exp}$	0.45[43]	NA
$\eta_{vol,pump}$	0.8[43]	NA
$\beta_{\eta v}$	0.36	NA
β_{Vol}	0.5[43]	NA
β_{ω}	0.2[43]	NA

simulations for the devices in the amine-scrubbing and CO_2 compression facilities.

CO_2 compression stage

The CO_2 is stored as a liquid to reduce its volume. To achieve this condition, the CO_2 will be compressed from 1 bar to 75 bar (11-12, Fig. 1) with two cooling stages until it reaches 29°C. In the first cooling stage, the CO_2 releases heat to the ORC (12-13, Fig. 1), and in the second stage, the CO_2 is cooled with atmospheric air under standard conditions (13-14-15-16 Fig. 1). Finally, the CO_2 is stored in a tank, as seen in Fig. 1.

Organic cycle Rankine

Working fluid selection

Cyclopentane (C_5H_{10}) has been selected as a working fluid in the ORC. This working fluid (WF) has had excellent results in previous ORC research on ICEs.[44] Also, it is thermally stable at temperatures up to 350°C.[45] Another extensive factor for its selection is that C_5H_{10} has a limited environmental impact, low toxicity and is noncorrosive.[46]

ORC configuration

The configuration of the ORC was made following the procedure developed by Fatigati *et al.*[43,47] This procedure calculates the maximum inlet pressure in the expander using Eqn 2.

$$P_{in,ex} = ZR\left(T_{sat} + \Delta T_{SH}\right)\rho_{pmp,in}\beta_{\eta v}\beta_{Vol}\beta_{\omega} \quad (2)$$

This equation relates the inlet condition in the expander and pump of the ORC through dimensionless variables: $\beta_{\eta v}$ is the product of the volumetric efficiencies of the expander and pump; β_{Vol} is the ratio between the displacement volume of the pump and expander; and β_{ω} is the ratio between the rotational speed of the pump and the expander. Maximum inlet pressure also depends on the superheating temperature difference (ΔT_{SH}) that increases with the engine load. The rest of the parameters in Eqn 1 are summarised in Table 6.

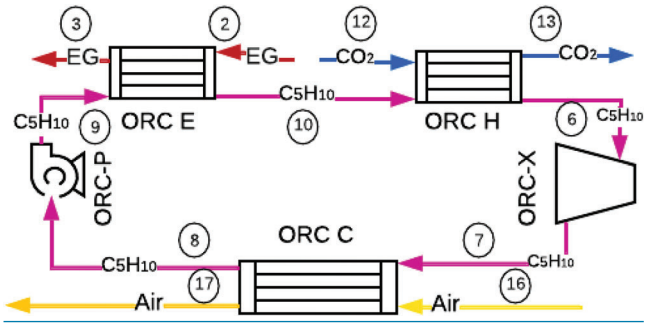

Figure 2. ORC layout used in the simulation.

For a pump inlet pressure of 1 bar, the maximum pressure obtained at the expander inlet is 9.05 bar. However, with the available heat in the exhaust gases after the stripper, the maximum saturation pressure achieved for the ORC cannot overcome 6.8 bar, whose value is less than the maximum allowed obtained with Eqn 2. So, the permeability value with 6.8 bar of expander inlet is 0.013 kg/MPa/s, which is a suitable permeability value according to the literature.[48]

With the values of low and high pressure found above, the ORC operation is under subcritical conditions. As there are two sources of heat (from the exhaust gases (2-3) and from the CO_2 after the compression process (12-13), Fig. 2), the ORC will have two evaporators (9-10-6, Fig. 2). The pressure drop value in the evaporators is 1.1 bar for each one, which is taken from the literature.[47] Finally, the ORC condenser cooling down the WF with air (7-8 and 16–17, Fig. 2), whose pressure drop is 0.2 bar.[47] This kind of ORC is called basic ORC (BORC).[49] Figure 2 displays the final configuration of the ORC, and Table 7 shows the values of the pressures and parameters considered for each device in the simulations.

Simulation of the hybridisation of the SI-ICE, CCS system and ORC

The amine scrubbing, CO_2 compression and ORC facilities were designed and modelled in Aspen plus. These systems have been integrated to use the residual heat in the exhaust gases in the desorption process and power production. Thus, to supply the power demand of the auxiliaries such as pumps and compressors considered in the simulations.

Figure 3 shows the hybridisation of the four systems mentioned above. Additional parameters are taken into account for the simulations: (i) concentration of the amine in the solvent is set to 30 wt%, (ii) mass fraction of the exhaust gases after the colling down process is 17.9% CO_2, 3% H_2O and 79.1% N_2, and (iii) the full line pressure of the amine-scrubbing facility is maintained between 1 and 1.1 bar. Table 8 summarises

Table 7. Equipment conditions for ORC simulations.

Equipment	Parameter	Unit	Value	State	Fluid
ORC-C	Inlet pressure	bar	1.2	Vapour	C_5H_{10}
	Overall heat transfer coefficient[50]	W/m^2K	500 Condensation	NA	Air- C_5H_{10}
ORC-P	Inlet pressure	bar	1	Saturated liquid	C_5H_{10}
	Isentropic efficiency	NA	0.55	NA	
ORC-H	Inlet pressure	bar	9	Compressed liquid	C_5H_{10}
	Overall heat transfer coefficient[50]	W/m^2K	150 Liquid-Gas	NA	C_5H_{10}–CO_2
ORC-E	Inlet pressure	bar	7.9	Compressed liquid	C_5H_{10}
	Overall heat transfer coefficient[50]	W/m^2K	70 Liquid–Gas 3000 Phase change 35 Gas–Gas	NA	C_5h_{10} –exhaust gas
ORC-X	Inlet pressure	bar	6.8	Vapour	C_5H_{10}
	Isentropic efficiency	NA	0.65	NA	

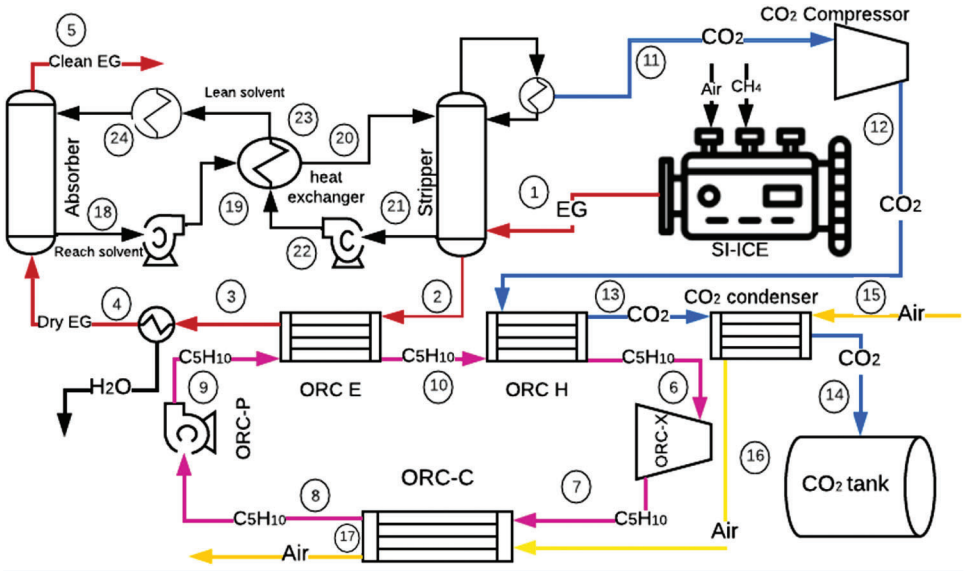

Figure 3. layout of the CCS system hybridised with the ORC.

Table 8. Thermal conditions of the fluids in the simulations.

Point	Fluid	Quality	Pressure (bar)	Temperature (°C)
1, 2, 3	Exhaust gases (EG)	1	1.09	*f(Engine load, rpm)*
4	EG	1	1.09	40
5	EG	*1*	1.09	*f(absorber process)*
6	C_5H_{10}	1	6.8	≥ 120
7	C_5H_{10}	*f(Engine load, rpm)*	1.2	*f(C_5H_{10} mass Flow)*
8	C_5H_{10}	0	1	49
9	C_5H_{10}	0	9	49
10	C_5H_{10}	*f(exhaust gases mass flow)*	7.9	122
11	CO_2	1	1	40
12	CO_2	1	75	565
13	CO_2	1	75	≥ 120
14	CO_2	0	75	29.3
15	Air	1	1	25
16	Air	1	1	*f(CO_2 mass flow)*
17	Air	1	1	*f(C_5H_{10} mass flow)*
18	Rich solvent	1	1	*f(absorber process)*
19	Rich solvent	1	1.1	*f(absorber process)*
20	Rich solvent	1	1.1	87
21	Lean solvent	1	1	118
22, 23,24	Lean solvent	1	1.1	*f(stripper process)*

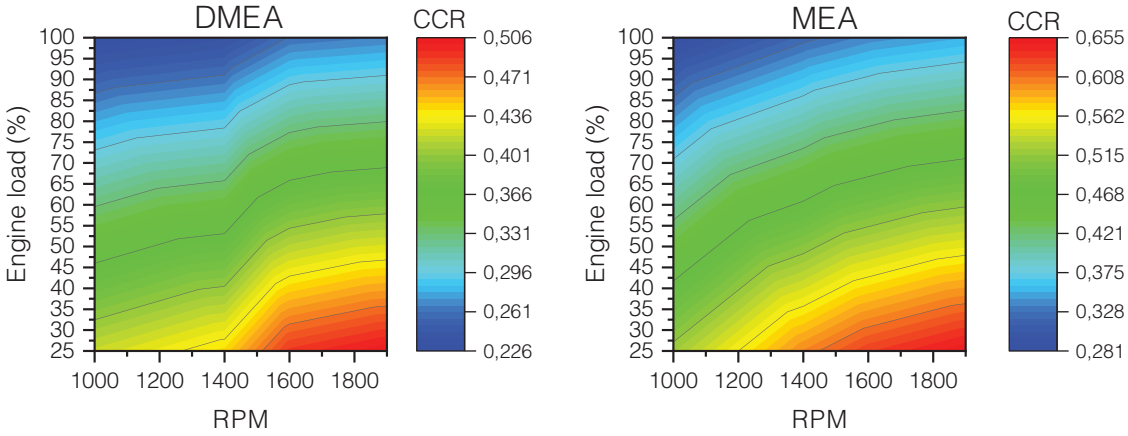

Figure 4. CCRs for MEA and MDEA over the entire rpm range and at partial engine loads.

all pressure and temperature values for each set point in the simulations. Since these parameters are established in the simulations, it proceeds to obtain the maximum CCR, the mass flow of solvent, WF and cooling air, as well as the power and thermal energy consumption of each device.

Results

Amine capture

Figure 4 shows the CCRs obtained in the amine-scrubbing facility with the two amines selected at partial engine load in the entire rpm range. There, it can be observed that the highest CCRs occur at the lower engine load conditions and highest rpm, with values of 0.506 and 0.655 for MDEA and MEA, respectively. The lowest values of the CCRs are presented, at high engine load and lower rpm, with values of 0.226 for MDEA and 0.281 for MEA.

Comparing the two amines, the solvent with MEA captures 14.9% more than MDEA at its best operating condition (25% engine load and 1900 rpm) and 5.5% more at the worst working condition (100% engine load and 1000 rpm). The tendency with both amines is similar; they present a high CCR at low engine loads and higher rpm and a lower CCR at high engine loads and lower rpm. The reason is that the mass of CO_2 captured, and the heat duty are the same for every engine load at a specific rotational speed (despite the increase in the exhaust gases' mass flow related to the engine load). These only increase with engine rotational speed and not with the engine load.

The heat duty for each rpm was always set up at 25 % of engine load with the aim that the stripper could operate in the other engine load conditions. For this reason, the heat duty in the stripper is kept constant for both amines. Thus, the reaction rate constant controls the CO_2 capture. MEA has a higher reaction rate coefficient than MDEA and can react with more CO_2 in the absorber resulting in a higher solvent mass flow and CCR than MDEA. Regeneration heat is directly affected, as a lower mass of CO2 is captured for the same heat duty with MDEA, producing a regeneration heat 33% higher than with MEA in the entire rpm range. This behaviour is because the CO_2 mass captured and the heat duty increase with the same slope. Figures 5 and 6 show the behaviours described above.

ORC heat exchanger areas

In order to be sure that the ORC can operate under all engine rpm and load conditions, the areas of the ORC and CO_2 compression system heat exchangers were obtained at the extreme points. Maximum engine load and 1900 rpm for the condensers and minimum load condition and 1000 rpm for the areas of the evaporators were set. Table 9 shows the resulting areas in the simulations with each solvent.

As is shown in the previous results, the total heat exchanger area in the ORC is 0.741 m^2 with the MEA solution and 0.509 m^2 with MDEA. This difference is since there is less WF mass flow in the ORC with MDEA than MEA because there is less solvent in the amine-scrubbing facility. This situation produces less demand for cooling, whereby the CCS system operating with MDEA requires less air mass flow of cooling than with MEA. This behaviour can be seen in Fig. 7.

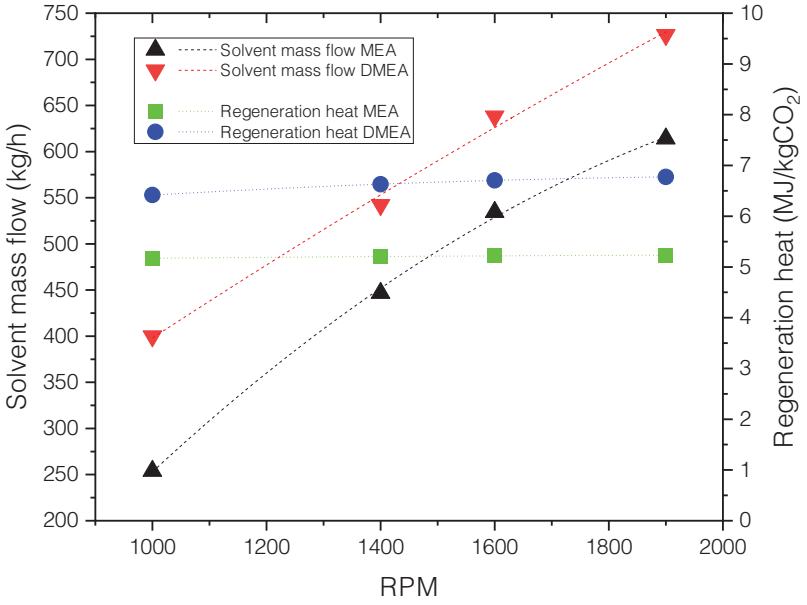

Figure 5. Solvent mass flow and regeneration heat for loading conditions.

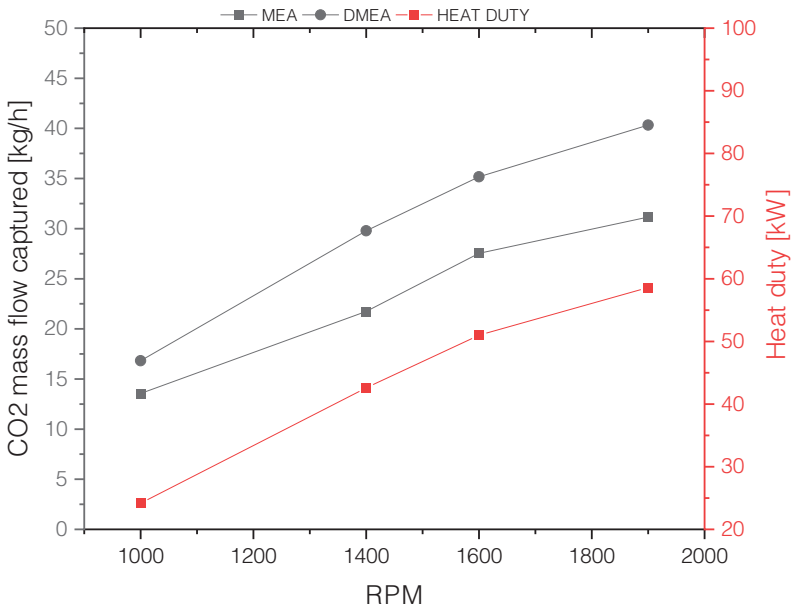

Figure 6. Heat duty in stripper and CO_2 mass capturer with the amine selected.

Energy analysis

The hybridisation of the ORC with the amine-scrubbing facility is done to further exploit the thermal energy available in the exhaust gases after the solvent regeneration process. This configuration tries to minimise the energy requirements of CO_2 storage, associated mainly with CO_2 compression. Figure 8 shows that the ORC thermal efficiency reaches a maximum of 11% at 1900 rpm and 25% engine load and a minimum of 8.6% at 1000 rpm and full engine load. This behaviour is the same with both solvents in the ORC, as it only depends on the available heat from the exhaust gases after the stripper. Values agree with those reported in the literature for the simulation of internal combustion engines operating with ORC.[48,51–53]

Table 9. Heat exchangers areas obtained in the simulations.

Amine	Heat exchanger	rpm	Engine load (%)	Exhaust gases mass flow (kg/h)	Area (m^2)	Variation (m^2)
MEA	Evaporator 1	1000	25	208.4	0.195	0.003
	Evaporator 2	1000	25	208.4	0.041	0.001
	ORC condenser	1900	100	754.7	0.361	0.0001
	CO_2 condenser	1900	100	754.7	0.144	0.002
MDEA	Evaporator 1	1000	25	208.4	0.143	0.004
	Evaporator 2	1000	25	208.4	0.033	0.002
	ORC condenser	1900	100	754.7	0.284	0.001
	CO_2 condenser	1900	100	754.7	0.109	0.003

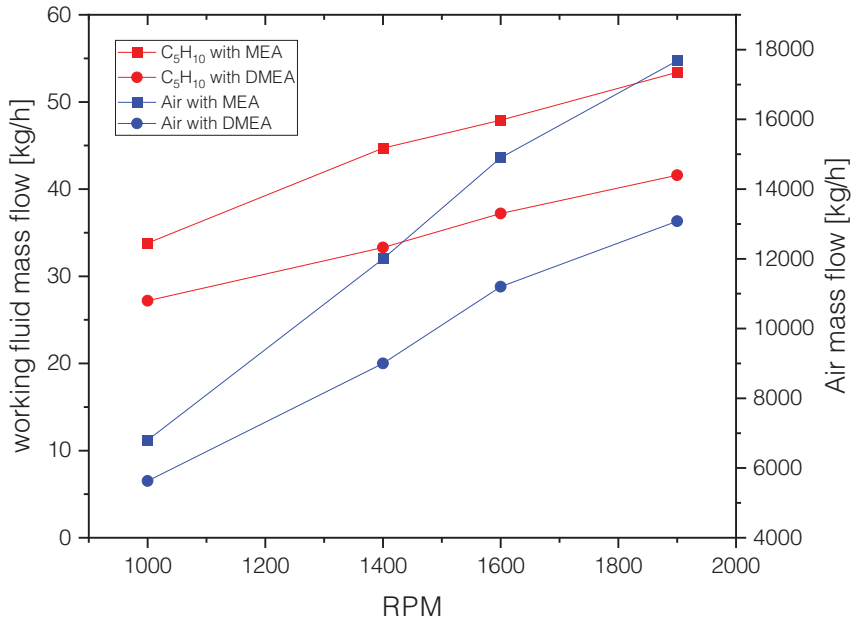

Figure 7. Working fluid and air mass flows in the ORC.

The penalisation power percentage on the engine performance is calculated by adding the power ORC expander, the CO_2 compression power and the powers of the ORC and CCS pumps and dividing all this by the engine power (Eqn 3).

$$\text{Power percentage} = \frac{-\dot{W}_{ORC-X} + \dot{W}_{ORC-P} + \dot{W}_{Pump1} + \dot{W}_{Pump2} + \dot{W}_{CO_2-compressor}}{BP} \quad (3)$$

Figure 9 shows that the CCS system with MEA and working with the ORC has a penalisation on the engine at its most critical point of 10.1%, while with MDEA, it is 8%. The difference is that more CO_2 is captured with MEA, so more CO_2 compression power is required. However, the simulations of the CCS system without ORC produce a penalisation on the engine power on average 1.5% higher than the CCS system with ORC for both solvents. In contrast, at the lowest point, the penalisation of the engine power is hardly noticeable.

Economic analysis

The economic analysis of the entire CCS is carried out with and without ORC for MEA and only with ORC for MDEA. Devices costs are obtained through equations found in the la literature. The total capital investment (CAPEX) is completed after including the direct and

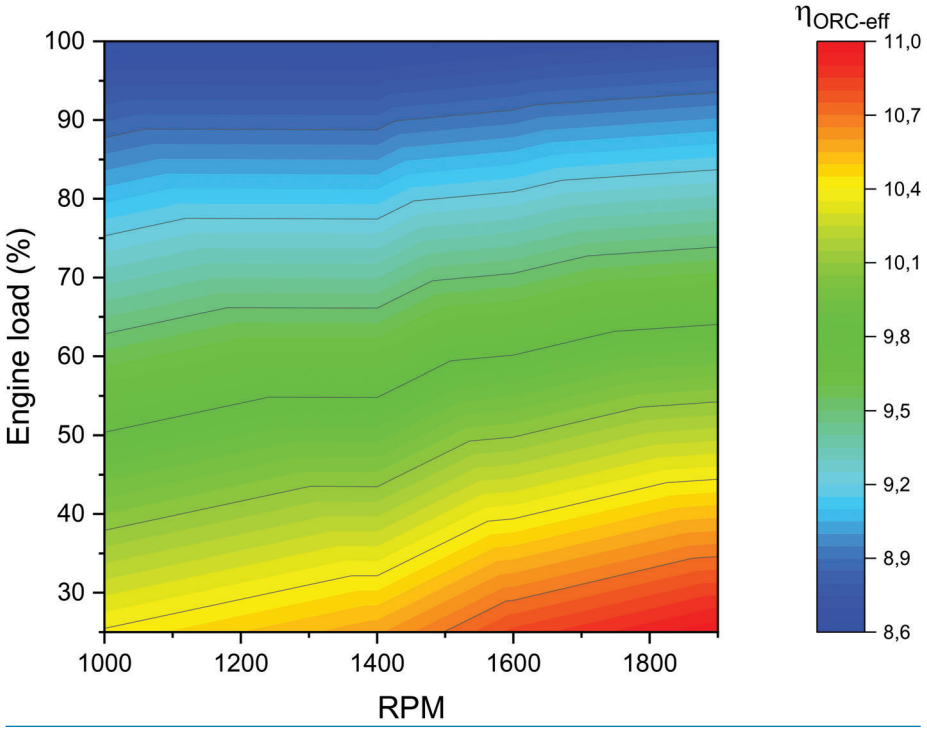

Figure 8. ORC efficiency over the entire engine rpm range and engine load conditions.

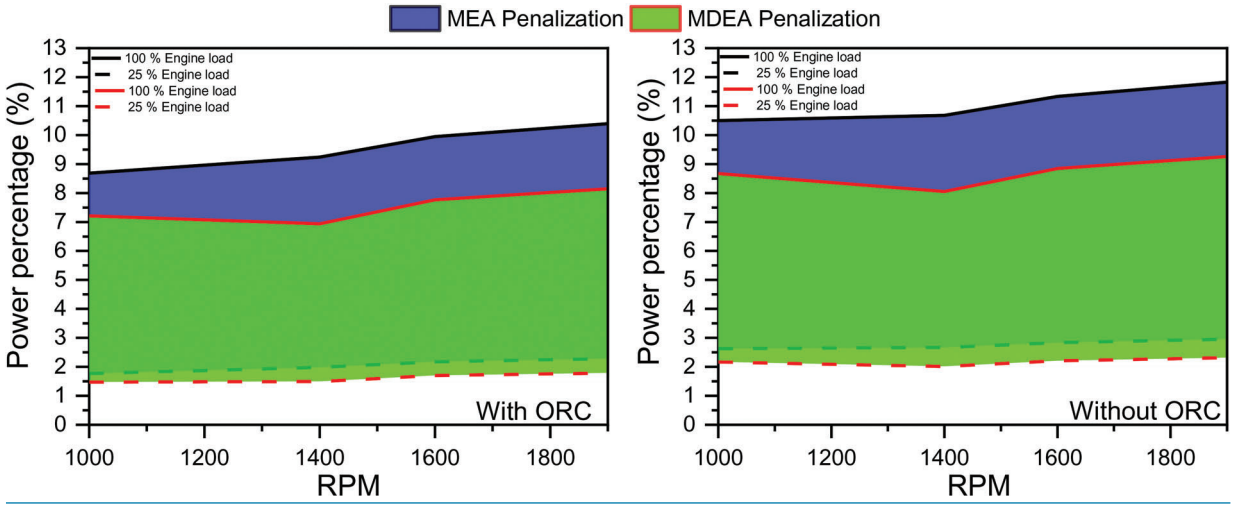

Figure 9. Percentage of power penalised of the engine by the CCS system with and without ORC.

indirect costs. Table 10 shows the equations used to calculate the CAPEX of the CCS system with the unit of waste heat recovery. The result is added to the value of an NG-fuelled bus, and they are compared with other commercial buses with CO_2 reduction technologies.

Figure 10 shows the percentage of the different items taken into account in the CAPEX and the total investment of the CCS system. It can be seen that amine plant cost has a weight greater than 50% in the three cases, while the importance of the ORC cost over the total is between 9.5 and 10.7%, depending on the amine used in the amine plant. As mentioned above, this is due to the size of the heat exchangers and compressor of CO_2.

The results show that with MEA, the CAPEX is 14.3 k€ higher than with MDEA. This difference is because the CCS system with MEA has a higher CCR than MDEA, requiring larger devices, which increases its

Table 10. CO_2 capture equipment installation costs CAPEX.

Process	Equipment	Cost equation	Parameter (A)	Ref.
Amine plant	All equipment's	26.094×106(A/408)0.65	CO_2 captured (t/h)	54, 55
ORC	ORC-X	1.5(225+170A)	Volume (m^3)	56
	ORC-P	900(A/300)0.25	Power (kW)	57
	ORC-fan	900(A/300)0.25	Power (kW)	
	ORC-C_5H_{10} tank	31.5+16A	Volume (L)	
	ORC-Evaporator	190+310A	Area (m^2)	
	ORC-H	190+310A	Area (m^2)	
	ORC-C	190+310A	Area (m^2)	
CO_2 storage system	Condenser	190+310A	Area (m^2)	57
	Compressor	267000(A/445)0.67	Power (kW)	58
	CO_2 tank	31.5+16A	Volume (L)	57
Direct cost	Installing	8%A	Amineplant+ORC+CO_2 storage system	Own criterion
	Instrumentation	5%A		
	Piping	1.5%A		
	Electric installing	1%A		
Indirect cost	Engineering	7%A	Amineplant+ORC+CO_2 storage system+ direct cost	54
	Contingency	8%A		

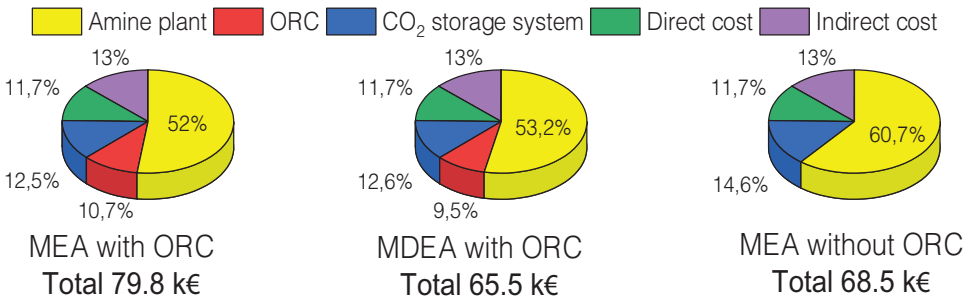

Figure 10. Total CAPEX and percentage weight of each item included in the CAPEX.

cost. The CAPEX of the capture system without ORC using MEA is 14.1% lower regarding the base case. To conclude the economic viability of a bus with a CCS system, a search of bus prices that using different CO_2 reduction technologies such as hydrogen fuel cell buss (HFCB) and electric battery (EB) bus has been done. Table 11 shows the bus prices found.

According to the bus prices shown in Table 11, diesel bus is still the best alternative when it comes to the initial investment, as they are 8.5% cheaper than the base case. However, it is well known that high pollutant emissions, mainly particulate matter and nitrogen oxide emissions, are the Achilles heel of diesel buses. On the other hand, it is observed that the price of a bus with a CCS is about 40 percentage points below that of hydrogen fuel cell and battery-electric buses.

From the obtained data, installing a capture system increases the cost of the CNG-fuelled bus by 18.3–21.3%. However, when the transport sector must pay for carbon Permits, the CCS in ICEv and the fuel cell system will be the best choice for the conventional vehicle. Based on the above, the fuel cell bus becomes more relevant because it does not emit CO_2. In the second place, it would be the vehicle with a capture system as it would achieve a CO_2 reduction of up to 66%, making it much more competitive than its conventional diesel counterpart. However, CCR is not enough to reach a totally CO_2-neutral system, unlike electric and hydrogen cell vehicles. Nevertheless, a bus

Table 11. Purchase of passenger transport buses in euros.

Technology or fuel	Value (k€)	Difference from the base case (%)	Reference
Compressed NG (CNG)	374.6	0.0	59, 60
Diesel	342.9	8.5	60
HFCB	650	–73.5	61
EB	604	–61.2	62
CNG+CCS+ORC	454.4	–21.3	This study
CNG+CCS	443.1	–18.3	This study

with a CCS system with a 1 m^3 storage tank at the conditions set out in this study could have autonomy up to 600 km (calculated with fuel consumption of 0.68 kg/km[63]), which is 2.4 times longer than the current maximum range of commercial electric vehicles, which is 250 km on average.[64]

Conclusions

A thermo-economic study of onboard CO_2 capture using amine scrubbing of a vehicle powered by a spark-ignition turbocharged internal combustion engine operating on natural gas has been carried out. According to the obtained results, the amine with the highest potential for CO_2 capture is MEA, having a higher CO_2 capture rate than MDEA under the whole range of engine operating conditions. However, the thermal integration of the exhaust gases with the CCS systems and ORC is technically feasible only for the CCS system. Because the exhaust gases can cover the desorption process of the CO_2 captured, but with the thermal energy reaming in the exhaust gases after the stripper, the ORC cannot produce enough power to reduce the penalisation on the performance engine. Also, incorporating an ORC into the capture system does not offer a real benefit in terms of energy and economy. On the contrary, it would add weight and volume to the bus, increasing the vehicle's operating and maintenance costs.

The present study provides a first approximation to the use of amines in onboard capture. It would also be necessary to conduct detailed research on the reaction of amines with other pollutants in the exhaust gases, absorber and stripper sizing and engine operation problems due to the resistance offered by the systems to the exhaust gases detrimental to engine performance.

Although this type of application in the transport sector is still in its initial research phase, the thermo-economic results obtained in this research show that a CCS by amine scrubbing with MEA and without ORC can become a competitive alternative to BEV and FCV, in particular in long distances. These capture-equipped vehicles will bring the transport sector closer to meeting the CO_2 reduction targets set by the European Union.

References

1. Kouridis C, Vlachokostas C. Towards decarbonising road transport: Environmental and social benefit of vehicle fleet electrification in urban areas of Greece. Renewable Sustainable Energy Rev. 2022;153:111775.
2. Auer M, Ganzer G, Müller-Baum P, Stiesch G. Synthetic fuels in large engines - how internal combustion engines become CO_2-neutral. MTZ Worldwide. 2019;80(3):48–51.
3. L'Orange Seigo S, Dohle S, Siegrist M. Public perception of carbon capture and storage (CCS): a review. Renewable Sustainable Energy Rev. 2014;38:848–63.
4. Rubin ES. Understanding the pitfalls of CCS cost estimates. Int J Greenhouse Gas Control. 2012;10:181–90.
5. García-Mariaca A, Llera-Sastresa E. Review on carbon capture in ICE driven transport. Energies. 2021;14:6865.
6. Leeson D, mac Dowell N, Shah N, Petit C, Fennell PS. A Techno-economic analysis and systematic review of carbon capture and storage (CCS) applied to the iron and steel, cement, oil refining and pulp and paper industries, as well as other high purity sources. Int J Greenhouse Gas Control. 2017;61:71–84.
7. Sullivan JM, Sivak M. Carbon capture in vehicles: a review of general support, available mechanisms, and consumer acceptance issues [Internet]. University of Michigan Transportation Research Institute; 2012. Available from: http://deepblue.lib.umich.edu/handle/2027.42/90951
8. Schmauss TA, Barnett SA. Viability of vehicles utilising on-board CO_2 capture. ACS Energy Letters. 2021;6:3180–4.
9. Awoyomi A, Patchigolla K, Anthony EJ. CO_2/SO_2 emission reduction in CO_2 shipping infrastructure. Int J Greenhouse Gas Control. 2019;88:57–70.
10. Stec M, Tatarczuk A, Iluk T, Szul M. Reducing the energy efficiency design index for ships through a post-combustion carbon capture process. Int J Greenhouse Gas Control. 2021;108(May 2020).
11. Güler E, Ergin S. An investigation on the solvent based carbon capture and storage system by process modeling and

comparisons with another carbon control methods for different ships. Int J Greenhouse Gas Control. 2021;110:103438.
12. Ros JA, Skylogianni E, Doedée V, van den Akker JT, Vredeveldt AW, Linders MJG, et al. Advancements in ship-based carbon capture technology on board of LNG-fuelled ships. Int J Greenhouse Gas Control. 2022;114:103575.
13. Luo X, Wang M. Study of solvent-based carbon capture for cargo ships through process modelling and simulation. Appl Energy. 2017;195:402–13.
14. Feenstra M, Monteiro J, van den Akker JT, Abu-Zahra MRM, Gilling E, Goetheer E. Ship-based carbon capture onboard of diesel or LNG-fuelled ships. Int J Greenhouse Gas Control. 2019;85(March):1–10.
15. Sharma S, Maréchal F. Carbon dioxide capture from internal combustion engine exhaust using temperature swing adsorption. Front Energy Res. 2019;7(December):1–12.
16. Kumar P, Rathod V, Parwani AK. Experimental investigation on performance of absorbents for carbon dioxide capture from diesel engine exhaust. Environ Prog Sustainable Energy. 2021;e13651.
17. Saravanan S, Kumar R. Experimental investigations on CO_2 recovery from engine exhaust using adsorption technology. SAE Technical Paper. 2019;28:2577.
18. Osorio-Tejada JL, Llera-Sastresa E, Scarpellini S. Liquefied natural gas: Could it be a reliable option for road freight transport in the EU? Renewable Sustainable Energy Rev. 2017;71:785–95.
19. Mottschall M, Kasten P, Rodríguez F. Decarbonization of on-road freight transport and the role of LNG from a German perspective. Öko-institut eV, International 2020, Berlin.
20. Mercedes-Benz. Citaro NGT technical information [Internet]. 2017 [cited 2020 Feb 8]. Available from: https://www.mercedes-benz-bus.com/content/dam/mbo/markets/common/buy/services-online/download-technical-brochures/images/content/regular-service-buses/citaro-ngt/MB-NGT-2-ES-09_17.pdf
21. Obiols J, Soleri D, Dioc N, Moreau M. Potential of concomitant injection of CNG and gasoline on a 1.6L gasoline direct injection turbocharged engine. SAE Technical Papers. 2011.
22. López JJ, Novella R, Gomez-Soriano J, Martinez-Hernandiz PJ, Rampanarivo F, Libert C, et al. Advantages of the unscavenged pre-chamber ignition system in turbocharged natural gas engines for automotive applications. Energy. 2021;218:119466.
23. Yontar AA, Doğu Y. Effects of equivalence ratio and CNG addition on engine performance and emissions in a dual sequential ignition engine. Int J Engine Res. 2020;21(6):1067–82.
24. Wu Y, Xu J, Mumford K, Stevens GW, Fei W, Wang Y. Recent advances in carbon dioxide capture and utilisation with amines and ionic liquids. Green Chemical Engineering. 2020;1(1):16–32.
25. Gouedard C, Picq D, Launay F, Carrette PL. Amine degradation in CO_2 capture. I. A review. Int J Greenhouse Gas Control. 2012;10:244–70.
26. Chowdhury FA, Yamada H, Higashii T, Goto K, Onoda M. CO_2 capture by tertiary amine absorbents: A performance comparison study. Ind Eng Chem Res. 2013;52(24):8323–31.
27. Romeo LM, Minguell D, Shirmohammadi R, Andrés JM. Comparative analysis of the efficiency penalty in power plants of different amine-based solvents for CO_2 capture. Ind Eng Chem Res. 2020;59(21):10082–92.
28. Cuccia L, Dugay J, Bontemps D, Louis-Louisy M, Vial J. Analytical methods for the monitoring of post-combustion CO_2 capture process using amine solvents: A review. Int J Greenhouse Gas Control. 2018;72:138–51.
29. Sada E, Hidehiro K, Butt MA. Gas absorption with consecutive chemical reaction: absorption of carbon dioxide into aqueous amine solutions chemical absorption mechanism. Can J Chem Eng. 1976;54(5):421–4.
30. Ali BS, Aroua MK. Effect of piperazine on CO_2 loading in aqueous solutions of MDEA at low pressure. Int J Thermophys. 2004;25(6):1863–70.
31. Hartono A, da Silva EF, Svendsen HF. Kinetics of carbon dioxide absorption in aqueous solution of diethylenetriamine (DETA). Chem Eng Sci. 2009;64(14):3205–13.
32. Hikita H, Asai S, Katsu Y, Ikuno S. Absorption of carbon dioxide into aqueous monoethanolamine solutions. AIChE J. 1979;25(5):793–800.
33. el Hadri N, Quang DV, Goetheer ELV, Abu Zahra MRM. Aqueous amine solution characterisation for post-combustion CO_2 capture process. Appl Energy. 2017;185:1433–49.
34. Kim YE, Lim JA, Jeong SK, Yoon Y, Il, Bae ST, Nam SC. Comparison of carbon dioxide absorption in aqueous MEA, DEA, TEA, and AMP solutions. Bull Korean Chem Soc. 2013;34(3):783–7.
35. Chen X, Rochelle GT. Aqueous piperazine derivatives for CO_2 capture: accurate screening by a wetted wall column. Chem Eng Res Des. 2011;89(9):1693–710.
36. Bishnoi S, Rochelle GT. Absorption of carbon dioxide into aqueous piperazine: Reaction kinetics, mass transfer and solubility. Chem Eng Sci. 2000;55(22):5531–43.
37. Wang Y, Zhao L, Otto A, Robinius M, Stolten D. A review of post-combustion CO_2 capture technologies from coal-fired power plants. Energy Procedia. 2017;114(November 2016):650–65.
38. Derks PWJ, Versteeg GF. Kinetics of absorption of carbon dioxide in aqueous ammonia solutions. Energy Procedia. 2009;1(1):1139–46.
39. Fu K, Sema T, Liang Z, Liu H, Na Y, Shi H, et al. Investigation of mass-transfer performance for CO_2 absorption into diethylenetriamine (DETA) in a randomly packed column. Ind Eng Chem Res. 2012;51(37):12058–64.
40. Kim YE, Moon SJ, Yoon Y Il, Jeong SK, Park KT, Bae ST, et al. Heat of absorption and absorption capacity of CO_2 in aqueous solutions of amine containing multiple amino groups. Sep Purif Technol. 2014;122:112–8.
41. Nakagaki T, Yamabe R, Furukawa Y, Sato H, Yamanaka Y. Experimental evaluation of temperature and concentration effects on heat of dissociation of CO_2-loaded MEA solution in strippers. Energy Procedia. 2017;114:1910–8.
42. Sønderby TL, Carlsen KB, Fosbøl PL, Kiørboe LG, von Solms N. A new pilot absorber for CO_2 capture from flue gases: measuring and modelling capture with MEA solution. Int J Greenhouse Gas Control. 2013;12:181–92.
43. Fatigati F, di Battista D, Cipollone R. Permeability effects assessment on recovery performances of small-scale ORC plant. Appl Therm Eng. 2021;196:117331.
44. Invernizzi CM, Iora P, Manzolini G, Lasala S. Thermal stability of n-pentane, cyclo-pentane and toluene as working fluids in organic Rankine engines. Appl Therm Eng. 2017;121:172–9.

45. Invernizzi CM, Bonalumi D. Thermal stability of organic fluids for organic Rankine cycle systems. Organic Rankine cycle (ORC) power systems: technologies and applications. Elsevier; 2017. p. 121–51.
46. Scaccabarozzi R, Tavano M, Invernizzi CM. Comparison of working fluids and cycle optimisation for heat recovery ORCs from large internal combustion engines. Energy. 2018;158:396-416
47. Fatigati F, di Bartolomeo M, di Battista D, Cipollone R. Experimental and numerical characterization of the sliding rotary vane expander intake pressure in order to develop a novel control-diagnostic procedure. Energies (Basel). 2019;12(10):1970.
48. Fatigati F, di Bartolomeo M, di Battista D, Cipollone R. Experimental characterisation of a hermetic scroll expander operating in an ORC-based power unit bottoming an internal combustion engine. In: AIP Conference Proceedings. American Institute of Physics Inc.; 2019.
49. Peris B, Navarro-Esbrí J, Molés F. Bottoming organic Rankine cycle configurations to increase internal combustion engines power output from cooling water waste heat recovery. Appl Therm Eng. 2013;61(2):364–71.
50. Kind M, Martin H. VDI Heat atlas. Second. Berlin: Springer; 2010. p. 1–1609.
51. Badescu V, Aboaltabooq MHK, Pop H, Apostol V, Prisecaru M, Prisecaru T. Design and operational procedures for ORC-based systems coupled with internal combustion engines driving electrical generators at full and partial load. Energy Convers Manage. 2017;139:206–21.
52. Shu G, Zhao M, Tian H, Wei H, Liang X, Huo Y, et al. Experimental investigation on thermal OS/ORC (Oil Storage/Organic Rankine Cycle) system for waste heat recovery from diesel engine. Energy. 2016;107:693–706.
53. Hoang AT. Waste heat recovery from diesel engines based on organic Rankine cycle. Appl Energy. 2018;231(March):138–66.
54. Abu-Zahra MRM, Niederer JPM, Feron PHM, Versteeg GF. CO_2 capture from power plants. Part II. A parametric study of the economical performance based on mono-ethanolamine. Int J Greenhouse Gas Control. 2007;1(2):135–42.
55. Bailera M, Espatolero S, Lisbona P, Romeo LM. Power to gas-electrochemical industry hybrid systems: A case study. Appl Energy. 2017;202:435–46.
56. Astolfi M. Techno-economic optimization of low temperature CSP systems based on ORC with screw expanders. Energy procedia; 2015:1100–12.
57. Quoilin S, Declaye S, Tchanche BF, Lemort V. Thermo-economic optimisation of waste heat recovery organic Rankine cycles. Appl Therm Eng. 2011;31(14–15):2885–93.
58. De Saint Jean M, Baurens P, Bouallou C, Couturier K. Economic assessment of a power-to-substitute-natural-gas process including high-temperature steam electrolysis. Int J Hydrogen Energy. 2015;40(20):6487–500.
59. Ally J, Pryor T. Life cycle costing of diesel, natural gas, hybrid and hydrogen fuel cell bus systems: an Australian case study. Energy Policy. 2016;94:285–94.
60. Holland SP, Mansur ET, Muller NZ, Yates AJ. The environmental benefits of transportation electrification: urban buses. Energy Policy. 2021;148.
61. Spendelow J, Papageorgopoulos D, Satyapal S. Fuel Cell Technologies Program Record 12012: Fuel Cell Bus Targets. 2012.
62. Quarles N, Kockelman KM, Mohamed M. Costs and benefits of electrifying and automating bus transit fleets. Sustainability. 2020;12(10):3977.
63. Stempien JP, Chan SH. Comparative study of fuel cell, battery and hybrid buses for renewable energy constrained areas. J Power Sources. 2017;340:347–55.
64. Wenz KP, Serrano-Guerrero X, Barragán-Escandón A, González LG, Clairand JM. Route prioritisation of urban public transportation from conventional to electric buses: A new methodology and a study of case in an intermediate city of Ecuador. Renewable Sustainable Energy Rev. 2021;148:111215.

Alexander García-Mariaca

Alexander García-Mariaca is a PhD candidate at Zaragoza University in renewable energy and energy efficiency. Alex's research focuses on the CO_2 capture process in mobile sources. He also has researched in performance and emissions of internal combustion engines, fluids dynamics, heat transfer, turbomachinery and mathematical modelling.

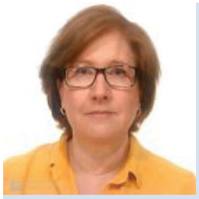

Eva Llera-Sastresa

Eva Llera-Sastresa is an Associate Professor in the Thermal Machines and Engines Area at the University of Zaragoza (Spain). Her research experience covers 20 years and has focused on two parallel research lines: energy socioeconomics and energy sustainability in activity sectors.